Explaining Regiodivergent Vinylations with Vinylbenziodoxolones**

Ester M. Di Tommaso, Per-Ola Norrby, and Berit Olofsson

Abstract: Vinylbenziodoxolones have recently been identified as efficient hypervalent iodine(III) reagents for electrophilic vinylations under transition metal-free conditions. Their unique reactivity allows synthesis of either internal or terminal alkenes, depending on the nucleophile class. This paper constitutes the first mechanistic investigation of VBX vinylations, and makes use of NMR studies, deuterium labelling and computations to rationalize the observed regio- and stereochemical outcome. Internal alkene formation in S-vinylation was found to proceed through the ligand coupling mechanism typical of diaryliodonium salts, whereas terminal alkene formation in P-vinylations took place via a phosphinous acid-coordinated VBX complex, which underwent concerted deprotonation and Michael-type addition. Subsequent base-assisted protonation and E2 elimination delivered the terminal alkene. The findings can be used to predict the regioselectivity in vinylations of other nucleophile classes.

Introduction

Alkenes are versatile building blocks in polymer chemistry, organic synthesis and drug discovery, and are biologically relevant functionalities common in pharmaceuticals.[1] Regiochemical control for selective synthesis of either the terminal or internal alkene, as well as stereochemical control of the *E/Z*-selectivity in internal alkenes is of paramount importance in many applications.[2] Hence, many regio- and stereoselective strategies to access alkenes have been developed over the past decades and generally involve

[*] E. M. Di Tommaso, Prof. B. Olofsson
Department of Organic Chemistry,
Arrhenius Laboratory, Stockholm University
10691 Stockholm (Sweden)
E-mail: berit.olofsson@su.se
Homepage: http://www.organ.su.se/bo/

Prof. P.-O. Norrby
Data Science and Modelling, Pharmaceutical Sciences, R&D,
AstraZeneca, Gothenburg (Sweden)

[**]A previous version of this manuscript has been deposited on a preprint server (https://doi.org/10.26434/chemrxiv-2022-q77mk).

transition metal-catalyzed cross coupling, C–H activation or metathesis.[2,3] With the increased focus on sustainable chemistry,[4] the development of transition metal-free, regio- and stereoselective alkenylations that proceed under mild conditions is highly important.[5]

Vinylbenziodoxolones (VBX) have recently been reported as novel hypervalent iodine(III) reagents sharing the same benziodoxolone core as the popular ethynylbenziodoxolones (EBX) and Togni reagents.[6] VBX compounds have already been employed as electrophilic vinylation reagents under transition metal-catalyzed, photocatalytic and metal-free conditions with a variety of nucleophiles (Scheme 1a).[7] VBX shows interesting reactivity under mild conditions without need for excess reagents, and tolerates a variety of functional groups. Core-substituted Me$_2$-VBX was reported to give improved results in some cases.[8] In parallel, the chemistry of β-heteroatom-substituted VBX reagents and their benziodoxole counterparts has also been developed.[9]
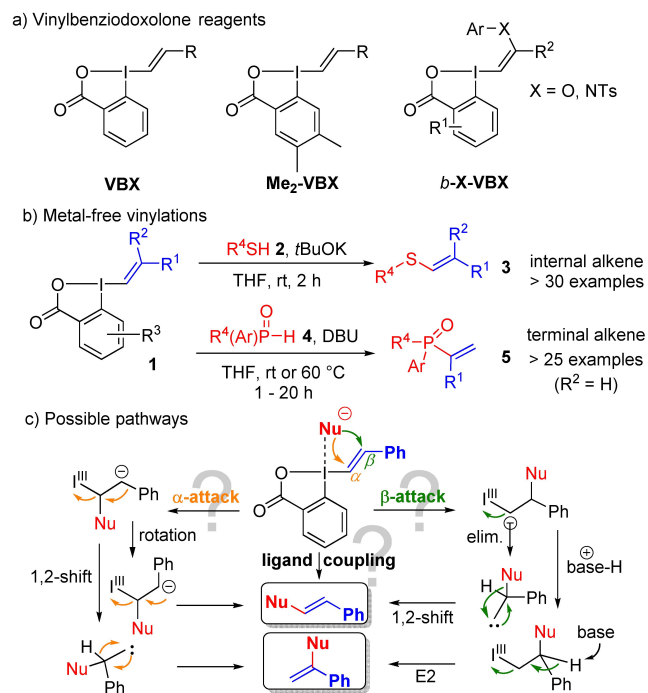
Methodology for transition metal-free vinylations from our lab highlights the intriguing reactivity of VBX reagents **1**. The efficient, room temperature S-vinylation of thiols **2** resulted in formation of internal alkenes **3** with retention of the VBX alkene configuration (Scheme 1b).[8–10] To the contrary, metal-free P-vinylation of phosphine oxides **4** or H-phosphinates delivered terminal alkenes **5** with complete

Scheme 1. Metal-free vinylations with VBX.

regioselectivity (Scheme 1b).[11] Terminal alkene formation was also favored with a C-nucleophile.[6a]

Literature reports of reactions with vinyl(aryl)iodonium salts, which are related iodine(III) reagents, indicate that various mechanisms can be operative under metal-free conditions. Vinylic S_N1 or S_N2 or reactions via alkylidene carbene intermediates are common, whereas Michael additions are less likely.[12] Vinylidene carbene formation has also been proposed in reactions with alkynyliodonium salts[13] and EBX.[14] Mechanistic studies of the latter revealed that thiol alkynylation can proceed via ligand coupling or Michael-type addition depending on the electronics of the reagent.[14]

To increase the utility of VBX as an efficient vinylating agent, tools to understand and predict the principles for product regiochemistry are important. Based on literature precedents, several possible mechanisms could be proposed to explain the observed regiochemistry (Scheme 1c). In this work, we have used NMR studies, deuterium-labelling and extensive DFT calculations of the S- and P-vinylations to unravel the mechanisms of VBX vinylations under transition metal-free conditions. Two mechanistic pathways are presented together with tools to predict the regiochemistry with other nucleophile classes.

Results and Discussion

S-Vinylation of Thiols

Earlier experimental observations were the starting point of this mechanistic study.[8] Vinylation of S-nucleophiles led exclusively to internal alkenes **3** ($E:Z$ ratio generally >20:1), indicating that VBX does not react through a vinylic S_N2 mechanism[15] (Scheme 1b). Alkenes **3** were formed also in the presence of radical traps. Furthermore, core-substituted Me2-VBX proved superior to the standard VBX as formation of disulfide $(ArS)_2$ byproduct was suppressed.[8]
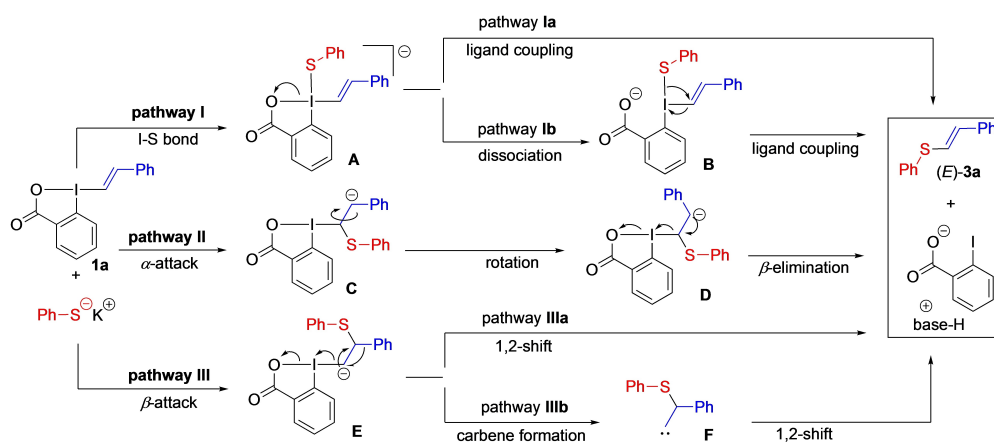
On account of experimental observations, literature mechanisms with vinyliodonium salts[12d] and the reported

mechanistic investigations of S-alkynylations with EBX,[10b,14,16] we proposed three possible pathways leading to (*E*)-**3a** and 2-iodobenzoate (Scheme 2). Thiophenol (**2a**) is first deprotonated by *t*BuOK, after which four-coordinated I–S intermediate **A** can form through ligand association (pathway **I**). This intermediate either undergoes direct ligand coupling to stereospecifically yield product (*E*)-**3a** (pathway **Ia**), or via release of the carboxylate ligand to intermediate **B** (pathway **Ib**).
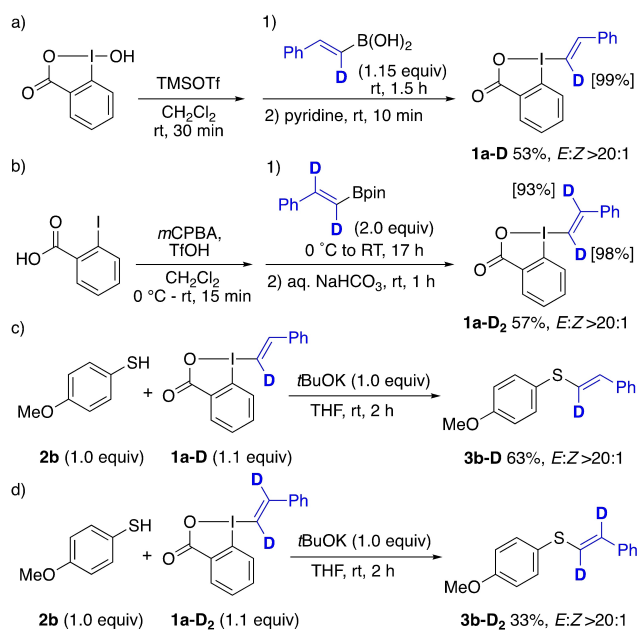
A direct nucleophilic attack on the α- or β-carbon of the vinyl moiety could also lead to product **3a**, although the (*E*)-selectivity could be compromised through such routes. Pathway **II** depicts an α-attack of the thiolate to yield intermediate **C**, which could rotate to intermediate **D** followed by β-elimination to give (*E*)-**3a**. Finally, attack on the β-carbon would give intermediate **E** via pathway **III**. This could undergo a concerted elimination and 1,2-shift of either the phenyl or sulfide moiety to yield vinyl sulfide **3a** directly (pathway **IIIa**), or stepwise elimination of iodobenzoate to yield alkylcarbene **F**, followed by a 1,2-shift (pathway **IIIb**). A concerted asynchronous alternative in between these two extremes is also possible.

We followed the reaction of VBX **1a** with **2a** in THF-d_8 by ^{1}H-NMR to investigate the formation of any intermediates and to rationalize the observed influence of the base addition order.[17] When **2a** was mixed with *t*BuOK in an NMR tube, signals of the thiophenolate were immediately observed and the vinylation started instantly when **1a** was added. A similar NMR experiment with **1a** and **2a** in the absence of base showed no interaction between the two, supporting our assumption that the thiophenolate forms prior to S–I coordination. The reaction started upon addition of the base, and thiophenolate was the only intermediate observed in both experiments.

To gain further understanding of the mechanism, deuterium-labelled VBX reagents **1a-D** and **1a-D₂** were synthesized (Scheme 3a,b).[6a,18] Thiophenol **2b** was employed as the model substrate to facilitate the NMR analysis of the reaction outcome. Reactions with **1a-D** under the standard conditions resulted in product **3b-D** as the only regioisomer, together with the corresponding disulfide by-

Scheme 2. Mechanistic pathways for S-vinylation with VBX.

Scheme 3. Deuterium-labelling study.

Figure 1. Reaction free energy profile [M06-2X(PCM)/def2-TZVP//M06-2X(PCM)/def2-SVP level in implicit THF solvent] for S-vinylation.

product in 11 % yield (Scheme 3c). The reaction with **1b-D₂** delivered product **3b-D₂** in moderate yield together with the disulfide byproduct (Scheme 3d). To reach these products through pathway **II**, complete selectivity in β-elimination from intermediate **D** rather than **C** would be needed, otherwise an *E:Z* mixture would be obtained.

DFT calculations were then performed at the M06-2X level of theory to investigate all three pathways. A low energy reaction profile was found for pathway **Ia**, starting with exothermic I–S bond formation to intermediate **A′** (Figure 1). The long bond lengths between the S–I and S–Cα atoms, (3.04 and 3.17 Å respectively) as well as the 167° S–I–C$_{aryl}$ angle, are similar to the tilted intermediate found in S-alkynylation with EBX.[14a] Ligand coupling through transition state **TS₁** leads stereospecifically to the vinylated product (*E*)-**3a** and iodobenzoate. The low energy of **TS₁** (18.2 kcal mol⁻¹) is in accordance with the experimentally observed high reaction rate at room temperature. Pathway **III** was found to be higher in energy by 13.7 kcal mol⁻¹, as depicted in Figure S15. Intermediates **B** and **C** could not be located; the structures converged to intermediate **A′**, indicating that the reaction proceeds through pathway **Ia**. We also computed the reaction profiles with Me₂-VBX **1b**, and *o*-Me-VBX **1c**, which resulted in very similar energies (Figures S13–S14). The benefit of reagent **1b** might be explained by the lower electrophilicity of the iodine compared to **1a**, thus resulting in cleaner reactions without formation of disulfide byproduct.

P-Vinylation of Phosphine Oxides

Contrary to the S-vinylation, the P-vinylation of diarylphosphine oxides **4** led exclusively to terminal alkenes **5** (Scheme 1b), and preliminary mechanistic studies revealed
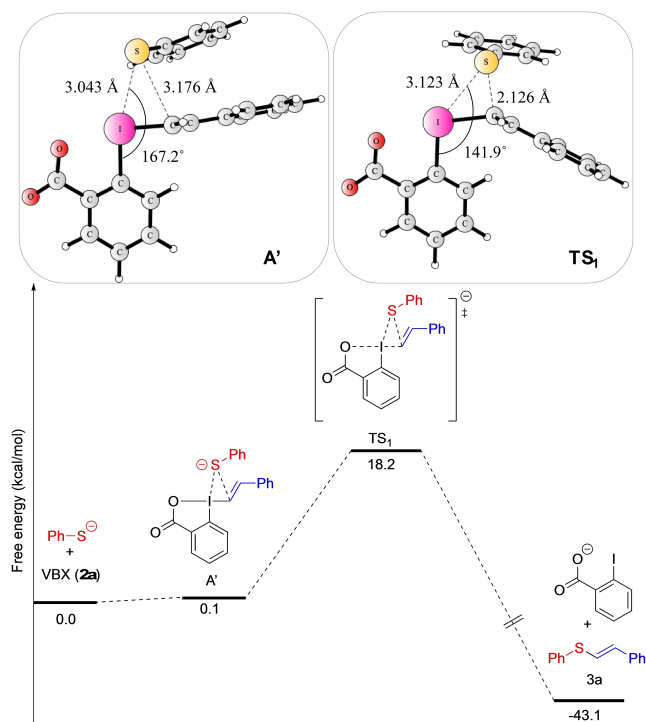
that a radical pathway was unlikely.[11] A ligand coupling mechanism can be ruled out, as this would lead to the internal alkene product. With inspiration from previous P-functionalizations with vinyl-[19] and alkynyliodonium salts,[20] and recent mechanistic studies with EBX,[14,21] we proposed five pathways leading to terminal alkene **5a** and 2-iodobenzoate (Scheme 4). In the presence of base, diphenyl-phosphine oxide (**4a**) and VBX **1a** can react through an α-attack to give intermediate **G**, which could undergo double 1,2-shifts to reach the terminal alkene **5a** via carbene **H** (pathway **IV**). Alternatively, the regioselectivity can be rationalized through a phospha-Michael-type reaction, which is a versatile and powerful tool for P–C bond formation.[22] Pathway **V** depicts a direct β-attack, yielding anionic intermediate **I**, which can form **5a** through three alternative pathways. Due to the high leaving group ability of the iodine(III) moiety, **I** could decompose to carbene **J**, which would yield **5a** through a 1,2-hydride shift. Alternatively, anion **I** could undergo a concerted 1,2-hydride shift and elimination to **5a**. Finally, protonation of intermediate **I** would give intermediate **K** with subsequent base-mediated β-elimination to **5a**. Alternatively, the four-coordinated I–P complex **L** forms prior to intramolecular Michael-type addition to yield intermediate **I** (pathway **VI**).

Phosphine oxide **4a** exists in equilibrium with the more reactive and nucleophilic phosphinous acid **4a′**,[23] which can participate in Michael additions under basic conditions.[22a,24] Pathway **VII** depicts deprotonation of **4a′** followed by reaction with **1a** to yield I–O bonded intermediate **M**, which is well aligned for a Michael-type addition to give **I**. In pathway **VIII**, **4a′** and **1a** instead form the weakly I–O
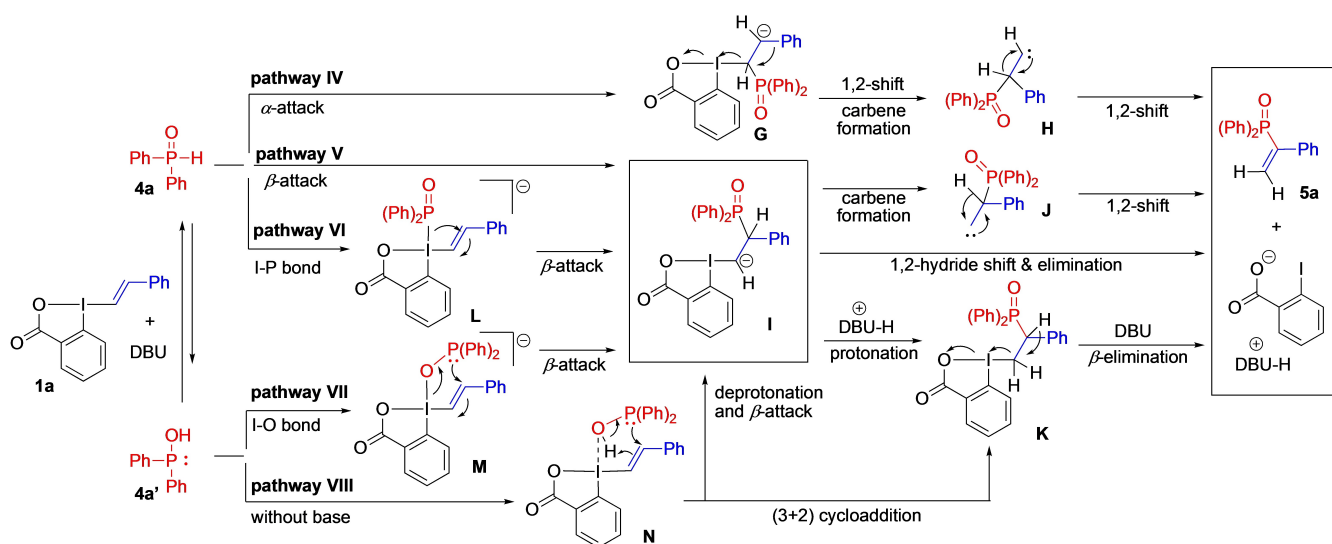
**Scheme 4.** Possible mechanistic pathways for P-vinylation with VBX.

coordinated intermediate **N**. This species could either undergo simultaneous deprotonation and β-attack to **I**, or undergo a (3+2) cycloaddition to intermediate **K**, followed by base-mediated β-elimination to **5a**.

NMR experiments in THF-d_8 were carried out to observe any reaction intermediates.[17] In the absence of VBX **1a**, no reaction was observed between DBU and **4a**. When **1a** was added, product **5a** started forming immediately, together with an intermediate that could later be identified (see below). Likewise, no adduct could be observed upon mixing **1a** and **4a** in the absence of DBU. These results indicate a simultaneous reaction between **1a**, **4a** and DBU rather than initial deprotonation of the nucleophile.

Deuterium-labelled VBX reagents **1a-D** and **1a-D₂** were utilized in a series of experiments to study whether any rearrangement or protonation took place (Scheme 5). The reaction of **4a** with **1a-D** delivered monodeuterated products **5a-D** in a 7:1 *Z*:*E* mixture as the only vinylation products observed (Scheme 5a). To verify these results, the reaction was repeated with *p*-methoxy-substituted phosphine oxide **4b** and **1a-D**, which simplified the NMR analysis (Figure S15–S17).

The vinylation of **4a** with **1a-D₂** resulted in a 1:1 mixture of **5a-D** isomers and no di-deuterated products were observed (Scheme 5b). A crossover experiment was performed with **1a-D₂** and **1d**, in which the expected products **5a-D** and **5c** were formed together with a trace amount of **5c-D** (Scheme 5c). Finally, deuterated phosphine oxide **4a-D** was employed with VBX **1a**, which resulted in the expected product **5a** as major product, with some deuterium incorporation to **5a-D**, now with the (*E*)-isomer as major isomer (Scheme 5d).

Based on these results, we propose that the reaction does not proceed through carbenes **H** or **J**, as these intermediates would give **5a-D₂** with reagent **1a-D₂**. Likewise, a concerted hydride shift and elimination from **I** is
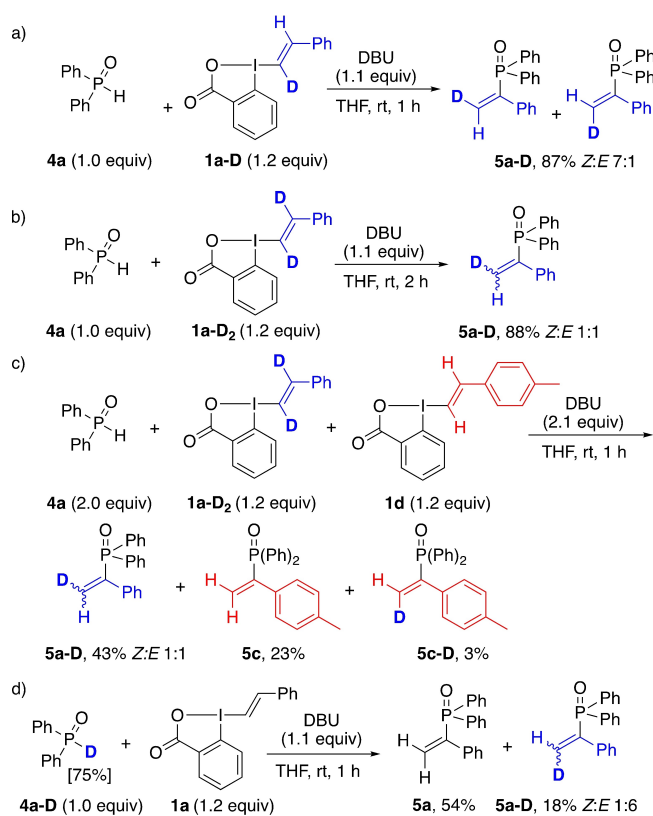
Scheme 5. Deuterium-labelling study.

ruled out. The results from Schemes 5c,d indicate that the base is involved in protonation, which aligns well with pathways **V–VIII** proceeding through intermediates **I** and **K**.

These pathways were analyzed in more detail to rationalize the observed stereoselectivity in formation of **5a-D** (Scheme 6). The reaction of phosphine oxide **4a** with **1a-D** would generate anionic intermediate **I–D**, which could either be protonated from above or below by ⁺DBU–H to
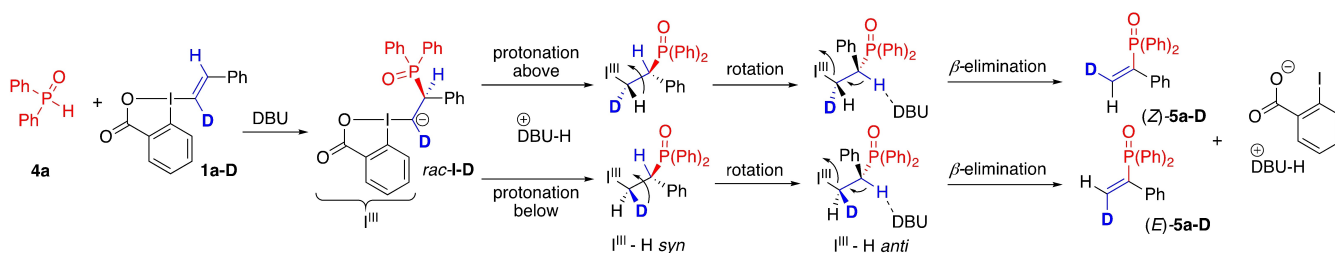
Scheme 6. Stereochemistry analysis with **1a-D**.

reach two diastereomeric intermediates. Rotation around the single bond to obtain *anti*-periplanar alignment followed by β-elimination yields (*Z*)-**5a-D** and (*E*)-**5a-D**, respectively. With the assumption that *anti*-elimination (E2) is favored over *syn*-elimination in this system, the observed high (*Z*)-selectivity in Scheme 5a indicates that protonation of **I–D** preferentially takes place from the same face as the phosphorous addition. This is also in agreement with the opposite stereoselectivity observed in Scheme 5d, where +DBU–D is used in the protonation step. The formation of **5a** as the major product in that reaction indicates that protonation with +DBU–H, which forms in the E2-elimination, is much faster than with +DBU–D. This is expected as a competitive proton/deuterium transfer should display a significant primary kinetic isotope effect.

DFT calculations were then performed to investigate the most plausible mechanisms in Scheme 4 based on the experimental observations. The lowest energy pathway was found to follow pathway **VIII** in Scheme 4, with isomerization of phosphine oxide **4a** to phosphinous acid **4a′** followed by formation of uncharged O–I intermediate **N′** with a hydrogen-bonded DBU molecule (Figure 2, **blue pathway**). Deprotonation proceeds simultaneously with the Michael addition via 5-membered **TS₁** (20.5 kcal mol⁻¹) as the rate determining step to give anionic intermediate **I′**. Protonation by +DBU–H preferentially takes place from above, to yield *syn*-**K′** (Figure S25), which rotates to *anti*-**K′**. As expected, subsequent E2-elimination is favored over the corresponding β-elimination from *syn*-**K′**, (Figure S26) and provides **5a** and 2-iodobenzoate. A direct (3+2) cyclo-
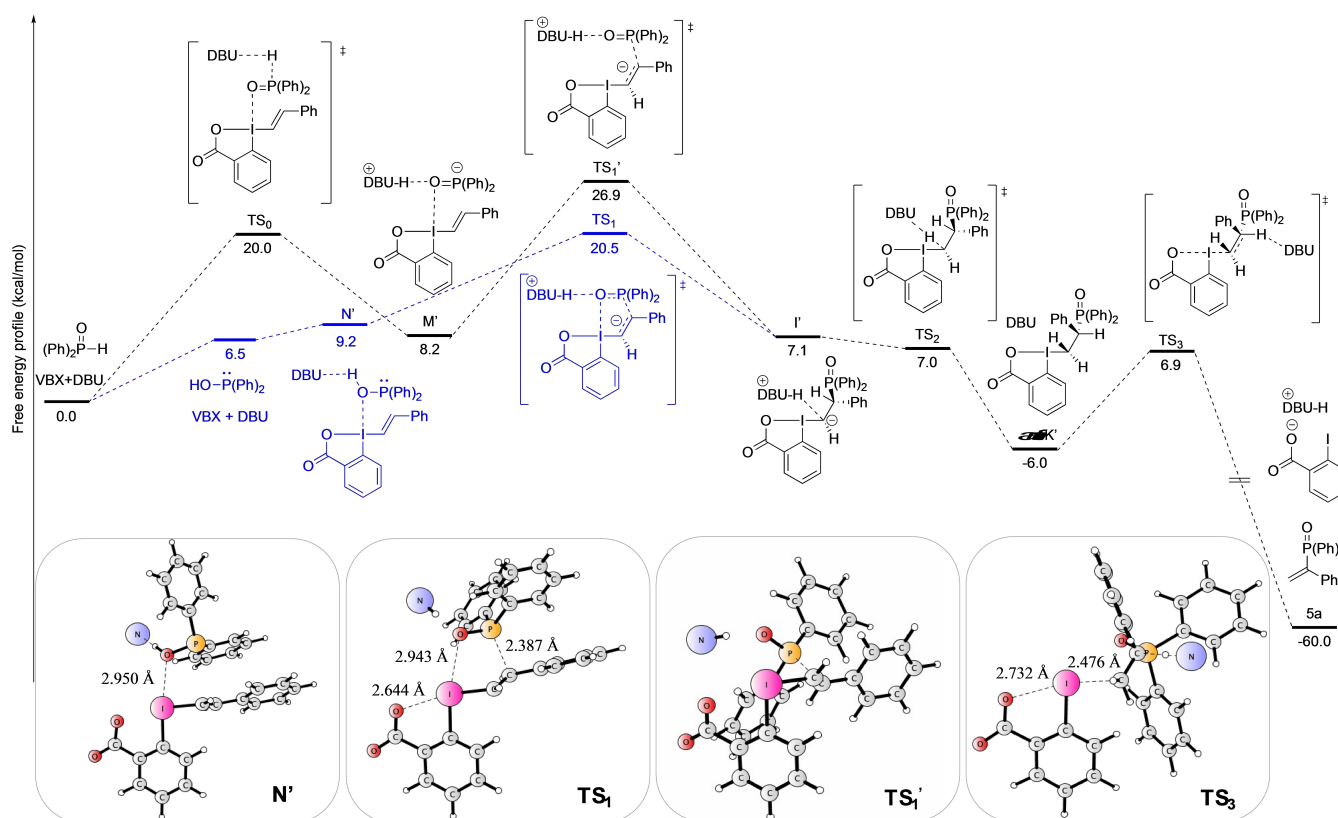

Figure 2. Simplified reaction free energy profile for P-vinylation. [M06-2X(PCM)/def2-TZVP//B3LYP-D3(PCM)/6-31g(d,p) + LANL2DZ level in implicit THF solvent] for P-vinylation mechanistic pathway. For clarity, 1,8-diazabiciclo[5.4.0]undec-7-en (DBU) is shown as a circled N and all atoms are omitted.

addition from **N′** to *anti*-**K′** was found to have a TS energy of 40.7 kcal mol^{-1} (Figure S31).

A low-energy pathway was also found roughly following pathway **VI**, where charged O–I intermediate **M′** is formed from phosphine oxide **4a** and **1a** via **TS$_0$** (Figure 2, **black pathway**). Coordination to the protonated base $^+$DBU–H stabilizes the partial negative charge on the oxygen. The mechanism proceeds by Michael-type addition via transition state **TS$_{1'}$** (26.9 kcal mol^{-1}) to anionic intermediate **I′**, after which the reaction proceeds as above. Computations of the other pathways from intermediate **I** in Scheme 4, including 1,2-hydride shift or carbene formation, revealed high-energy intermediates that are discussed in Figure S27 and S28.

Two ligand coupling pathways were investigated to support the observed complete regioselectivity for terminal over internal alkene product. The latter product could be formed through a 4-membered ligand coupling TS from O–I intermediate **M′** (Figure S23), or a three-membered ligand coupling TS via intermediate **L** (Figure S30), both with considerably higher TS energies than **TS$_1$** (Figure 2).

Further investigations were performed to support the formation of intermediate **K**. Upon shorter reaction time, the synthesis of **5a-D** from **4a** and **1a-D$_2$** was accompanied by isolation of another product, which was identified as compound **6-D$_2$** (Scheme 7). This finding was highly unexpected, as iodine(III) compounds with alkyl ligands are generally unstable.[25]

Compound **6-D$_2$** could be converted to product **5a-D** upon treatment with DBU, which supports that **K** is an intermediate in the reaction. Upon kinetic-NMR studies of reactions of **4a** with **1a**, the corresponding intermediate **6-H$_2$** could be detected in minor amounts (Figure S20). The varying $Z:E$ ratios obtained for **5a-D** can be explained by different selectivity in protonation of **I–D** vs. **I–D$_2$** from above or below, as the energy difference for *syn*- vs *anti*-elimination is much higher.

The mechanistic differences between VBX vinylations of thiols and phosphorus nucleophiles can be rationalized by invoking the preferential formation of a 5-membered TS over a 3-membered TS, which is generally required in ligand coupling mechanisms. This is in line with our previous findings in arylation of enolates with diaryliodonium salts, where a 5-membered pathway via an I–O intermediate was preferred over a 3-membered ligand coupling TS from the corresponding I–C intermediate.[26] Based on this conclu-

sion, other ambident nucleophiles would also be expected to coordinate to the iodine with subsequent Michael-type attack to yield terminal alkenes, whereas mono-nucleophilic species should give internal vinylation products. This is in line with the C-vinylation of nitrocyclohexanone, which gave the terminal product as the major regioisomer.[6a] Strong nucleophiles could prefer I–Nu coordination followed by ligand coupling or α-attack to give the internal product, as observed in vinylation of in situ-generated sulfenate anions.[10a] The possibility to control the regioselectivity by modulating the nucleophile structure should be of great interest in organic synthesis, and our continued studies of controlling VBX reactivity will be reported in due time.

Conclusion

A combined experimental and theoretical study of transition metal-free vinylations with the recently discovered hypervalent iodine(III) reagent VBX has revealed two different pathways leading either to the internal or the terminal alkene. Deuterium-labelling studies and computations support that the S-vinylation of thiols proceeds through deprotonation followed by a ligand coupling to provide the experimentally observed internal alkenes with retained *E*-configuration. The P-vinylation of diarylphosphine oxides instead begins with I–O coordination of the corresponding phosphinous acid to VBX. A simultaneous deprotonation and Michael-type addition then gives an anionic intermediate, which is transformed to the terminal alkene through a base-assisted protonation and E2 elimination. A general regioselectivity trend for VBX vinylations under metal-free conditions is predicted, where ambident nucleophiles will deliver terminal alkenes, whereas monodent or strong nucleophiles will provide internal alkenes.

Conflict of Interest
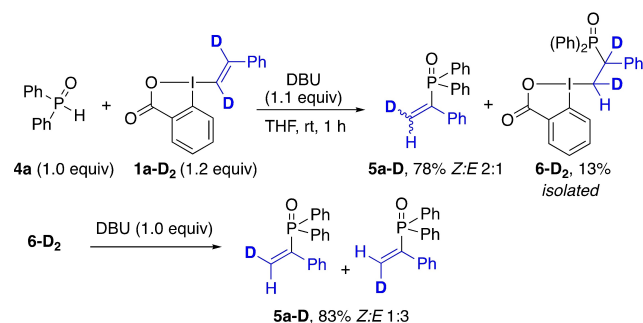
The authors declare no conflict of interest.

Data Availability Statement

The data that support the findings of this study are available in the supplementary material of this article.

Scheme 7. Support for iodine(III) intermediate **K**.

Angew. Chem. Int. Ed. **2022**, *61*, e202206347 (6 of 7)

© 2022 The Authors. Angewandte Chemie International Edition published by Wiley-VCH GmbH

[1] a) J. C. Mol, *J. Mol. Catal. A* **2004**, *213*, 39–45; b) K. C. Nicolaou, P. G. Bulger, D. Sarlah, *Angew. Chem. Int. Ed.* **2005**, *44*, 4490–4527; *Angew. Chem.* **2005**, *117*, 4564–4601.

[2] a) *Stereoselective Alkene Synthesis*, Springer, Berlin, Heidelberg, **2012**; b) A. B. Flynn, W. W. Ogilvie, *Chem. Rev.* **2007**, *107*, 4698–4745.

[3] a) C. C. C. Johansson Seechurn, M. O. Kitching, T. J. Colacot, V. Snieckus, *Angew. Chem. Int. Ed.* **2012**, *51*, 5062–5085; *Angew. Chem.* **2012**, *124*, 5150–5174; b) S. Tang, K. Liu, C. Liu, A. Lei, *Chem. Soc. Rev.* **2015**, *44*, 1070–1082; c) V. P. Boyarskiy, D. S. Ryabukhin, N. A. Bokach, A. V. Vasilyev, *Chem. Rev.* **2016**, *116*, 5894–5986; d) W. Ma, P. Gandeepan, J. Li, L. Ackermann, *Org. Chem. Front.* **2017**, *4*, 1435–1467; e) M. R. Becker, R. B. Watson, C. S. Schindler, *Chem. Soc. Rev.* **2018**, *47*, 7867–7881.

[4] K. Kümmerer, J. Clark, in *Sustainability Science: An Introduction* (Eds.: H. Heinrichs, P. Martens, G. Michelsen, A. Wiek), Springer Netherlands, Dordrecht, **2016**, pp. 43–59.

[5] C.-L. Sun, Z.-J. Shi, *Chem. Rev.* **2014**, *114*, 9219–9280.

[6] a) E. Stridfeldt, A. Seemann, M. J. Bouma, C. Dey, A. Ertan, B. Olofsson, *Chem. Eur. J.* **2016**, *22*, 16066–16070; b) T. Kitamura, T. Fukuoka, Y. Fujiwara, *Synlett* **1996**, 659–660.

[7] a) N. Declas, G. Pisella, J. Waser, *Helv. Chim. Acta* **2020**, *103*, 2000191; b) D. P. Hari, S. Nicolai, J. Waser, in *Patai's Chemistry of Functional Groups: The Chemistry of Hypervalent Halogen Compounds* (Eds.: B. Olofsson, I. Marek, Z. Rappoport), Wiley, Hoboken, **2019**, pp. 523–580.

[8] L. Castoldi, E. M. Di Tommaso, M. Reitti, B. Gräfen, B. Olofsson, *Angew. Chem. Int. Ed.* **2020**, *59*, 15512–15516; *Angew. Chem.* **2020**, *132*, 15642–15646.

[9] a) P. Caramenti, N. Declas, R. Tessier, M. D. Wodrich, J. Waser, *Chem. Sci.* **2019**, *10*, 3223–3230; b) J. Wu, X. Deng, H. Hirao, N. Yoshikai, *J. Am. Chem. Soc.* **2016**, *138*, 9105–9108; c) A. Yoshimura, C. D. Huss, M. Liebl, G. T. Rohde, S. M. Larson, G. B. Frahm, M. W. Luedtke, T. J. Schumacher, Z. S. Gardner, V. V. Zhdankin, P. S. Postnikov, M. S. Yusubov, T. Kitamura, A. Saito, *Adv. Synth. Catal.* **2021**, *363*, 3365–3371.

[10] See also this paper on S-vinylation: a) S. G. E. Amos, S. Nicolai, A. Gagnebin, F. Le Vaillant, J. Waser, *J. Org. Chem.* **2019**, *84*, 3687–3701; b) B. Liu, J. Alegre-Requena, R. Paton, G. Miyake, *Chem. Eur. J.* **2020**, *26*, 2386–2394.

[11] L. Castoldi, A. A. Rajkiewicz, B. Olofsson, *Chem. Commun.* **2020**, *56*, 14389–14392.

[12] a) M. Ochiai, K. Oshima, Y. Masaki, *J. Am. Chem. Soc.* **1991**, *113*, 7059–7061; b) M. Ochiai, Y. Kitagawa, M. Toyonari, K. Uemura, *Tetrahedron Lett.* **1994**, *35*, 9407–9408; c) T. Okuyama, T. Takino, T. Sueda, M. Ochiai, *J. Am. Chem. Soc.* **1995**, *117*, 3360–3367; d) M. Ochiai, *J. Organomet. Chem.* **2000**, *611*, 494–508.

[13] a) M. Ochiai, M. Kunishima, Y. Nagao, K. Fuji, M. Shiro, E. Fujita, *J. Am. Chem. Soc.* **1986**, *108*, 8281–8283; b) M. Ochiai, T. Ito, Y. Takaoka, Y. Masaki, M. Kunishima, S. Tani, Y. Nagao, *Chem. Commun.* **1990**, 118–119.

[14] a) R. Frei, M. D. Wodrich, D. P. Hari, P.-A. Borin, C. Chauvier, J. Waser, *J. Am. Chem. Soc.* **2014**, *136*, 16563–16573; b) M. D. Wodrich, P. Caramenti, J. Waser, *Org. Lett.* **2016**, *18*, 60–63.

[15] M. Ochiai, S. Yamamoto, T. Suefuji, D.-W. Chen, *Org. Lett.* **2001**, *3*, 2753–2756.

[16] R. Frei, T. Courant, M. D. Wodrich, J. Waser, *Chem. Eur. J.* **2015**, *21*, 2662–2668.

[17] See the Supporting Information for details.

[18] a) Z. He, A. K. Yudin, *J. Am. Chem. Soc.* **2011**, *133*, 13770–13773; b) A. Boelke, L. D. Caspers, B. J. Nachtsheim, *Org. Lett.* **2017**, *19*, 5344–5347; c) R. Shang, Z. Huang, L. Chu, Y. Fu, L. Liu, *Org. Lett.* **2011**, *13*, 4240–4243; d) Q. Feng, K. Yang, Q. Song, *Chem. Commun.* **2015**, *51*, 15394–15397.

[19] S. Thielges, P. Bisseret, J. Eustache, *Org. Lett.* **2005**, *7*, 681–684.

[20] J. S. Lodaya, G. F. Koser, *J. Org. Chem.* **1990**, *55*, 1513–1516.

[21] C. C. Chen, J. Waser, *Chem. Commun.* **2014**, *50*, 12923–12926.

[22] a) D. Enders, A. Saint-Dizier, M.-I. Lannou, A. Lenzen, *Eur. J. Org. Chem.* **2006**, 29–49; b) F. Palacios, C. Alonso, J. M. de los Santos, *Chem. Rev.* **2005**, *105*, 899–932.

[23] a) N. I. Ivanova, N. K. Gusarova, E. A. Nikitina, A. I. Albanov, L. M. Sinegovskaya, M. V. Nikitin, N. A. Konovalova, B. A. Trofimov, *Phosphorus Sulfur Silicon Relat. Elem.* **2004**, *179*, 7–18; b) D. Vincze, P. Ábrányi-Balogh, P. Bagi, G. Keglevich, *Molecules* **2019**, *24*, 3859.

[24] A. Christiansen, D. Selent, A. Spannenberg, M. Köckerling, H. Reinke, W. Baumann, H. Jiao, R. Franke, A. Börner, *Chem. Eur. J.* **2011**, *17*, 2120–2129.

[25] A. Yoshimura, V. V. Zhdankin, *Chem. Rev.* **2016**, *116*, 3328–3435.

[26] P.-O. Norrby, T. B. Petersen, M. Bielawski, B. Olofsson, *Chem. Eur. J.* **2010**, *16*, 8251–8254.